ELSEVIER

Biochimica et Biophysica Acta 1564 (2002) 91–98

BIOCHIMICA ET BIOPHYSICA ACTA
BBA

www.bba-direct.com

High-throughput screening of bacteriorhodopsin mutants in whole cell pastes

Lynell C. Martinez, George J. Turner*

Department of Physiology and Biophysics and the Neurosciences Program, The University of Miami School of Medicine, 1600 N.W. 10th Avenue, P.O. Box 016430, Miami, FL 33101, USA

Received 7 December 2001; received in revised form 14 March 2002; accepted 20 March 2002

Abstract

A high-throughput screening method has been developed which enables functional analysis of bacteriorhodpsin in whole cell pastes. Reflectance spectra, from as little as 5 ml of *Halobacterium salinarum* cells, show close correspondence to that obtained from the purified purple membrane (PM), containing bacteriorhodopsin (BR) as the sole protein component. We demonstrate accurate quantification of BR accumulation by ratiometric analysis of BR (A_{max} 568) and a membrane-bound cytochrome (A_{max} 410). In addition, ground-state light- and dark-adapted (LA and DA, respectively) spectral differences were determined with high accuracy and precision. Using cells expressing the BR mutant D85N, we monitored transitions between intermediate-state homologues of the reprotonation phase of the light-activated proton pumping mechanism. We demonstrate that phenotypes of three mutants (D85N/T170C, D85N/D96N, and D85N/R82Q) previously characterized for their effect on photocycle transitions are reproduced in the whole cell samples. D85N/T170C stabilizes accumulation of the N state while D85N/D96N accumulates no N state. D85N/R82Q was found to have perturbed the pK_a of M accumulation. These studies illustrate the correspondence between pH-dependent ground-state transitions accessed by D85N and the transitions accessed by the wild-type protein following photoexcitation. We demonstrate that whole cell reflectance spectroscopy can be used to efficiently characterize the large numbers of mutants generated by engineering strategies that exploit saturation mutagenesis.

Keywords: Bacteriorhodopsin; *Halobacterium salinarum*; Conformational equilibrium; Reflectance spectroscopy; High-throughput screening

1. Introduction

Bacteriorhodopsin (BR) is a light-activated proton pump expressed by the halophilic Archaeon, *Halobacterium salinarum* [1]. Owing to numerous experimental advantages, BR is one of the most extensively characterized membrane proteins. BR accumulates at very high levels in *H. salinarum,* up to 15 mg/l of cell culture [2,3]. At these levels of expression, wild-type BR forms specialized membrane patches referred to as purple membrane (PM), in which BR is the only protein [2]. The PM can constitute up to 50% of the *H. salinarum* membrane. The high protein-to-lipid ratio of PM causes these membrane patches to have a higher buoyant density than that of the surrounding membrane, and it can therefore be purified from the remaining membrane fraction by sucrose density centrifugation [2]. In addition, the packing of BR into PM results in the formation of two-dimensional crystalline lattices in vivo [4].

The ground-state structure of BR has been solved to atomic resolution and demonstrates that the tertiary structure is composed of seven α-helical transmembrane segments, with an extracellular amino terminus and a cytoplasmic carboxyl terminus [5–9]. An aldehyde of vitamin A (retinal) is covalently coupled to the ε-amino group of lysine 216, in the middle of the seventh helix, via a Schiff base linkage. Upon absorption of a photon, the retinal undergoes isomerization from the *all-trans* to the *13-cis* configuration [10] initiating a series of conformational changes that are coupled to the protonation and deprotonation of key amino acid residues. As the protein undergoes structural rearrangement,

Abbreviations: ATP, adenosine triphosphate; *bop*, bacterio-opsin gene; bp, base pair; BR, Bacteriorhodopsin; BTP, bis tris-propane; CAPS, (3-[cyclohexylamino]-1-propane-sulfonic acid); DA, dark-adapted; dNTP, deoxy-nucleoside triphosphate; *E. coli*, *Escherichia coli*; *H. salinarum*, *Halobacterium salinarum*; kb, kilobase pair; LA, light-adapted; λ_{max}, wavelength at absorbance maximum; nm, nanometer; oligo, oligo deoxy-nucleotide; PCR, polymerase chain reaction; PM, purple membrane harvested from sucrose-density gradients containing purified BR trimers

* Corresponding author. Tel.: +1-305-243-3189; fax: +1-305-243-5931.
E-mail address: gturner@miami.edu (G.J. Turner).

0005-2736/02/$ - see front matter
PII: S0005-2736(02)00406-6

the electrogenic environment of retinal changes, altering the spectral characteristics of BR. Using ground-state and time-resolved visible absorbance spectroscopy, seven spectrally distinct intermediates of BR have been identified ($BR_{568} \rightarrow J \leftrightarrow K_{630} \leftrightarrow L_{550} \leftrightarrow M1_{412} \rightarrow M2_{412} \leftrightarrow N_{550} \leftrightarrow O_{640} \rightarrow BR_{568}$) and the transitions between them extensively characterized [10–15]. Completion of the photo-induced structural transitions results in translocation of protons from the intracellular to the extracellular surface of the membrane [16]. Proton translocation produces an electrochemical gradient that is utilized for energy requiring cellular processes [17,18].

Proton pumping by BR can be divided into two phases, the deprotonation phase (BR through M1) and the reprotonation phase (M2 through BR), based on the accessibility of the Schiff base. Structural changes that determine the Schiff base accessibility occur in the M1 → M2 transition [14,19,20] and involve rearrangement of the F and G helices [8,9,21]. The protonation-state of Asp-85 plays a central role in the conformational changes and linked proton movements. D85 is protonated (from the Schiff base) during the formation of the M intermediate and remains protonated in the N and O intermediates [22–24]. Proton transfer from D85 to the proton release group (PRG) is the rate-limiting step in the O → BR transition of the photocycle [25]. Replacement of D85 with Asn (D85N) results in a protein that undergoes structural changes that regulate the pK_a's of D96 and the Schiff base in a manner consistent with that observed in the reprotonation phase of the wild-type protein. In the absence of photoexcitation, three spectrally distinct species exist in equilibrium and their accumulation is regulated by pH. At neutral pH, the protein exists, almost exclusively, in an O-like species ($\lambda_{max} = 615$ nm). As the pH is raised, two additional chromophoric species, an N-($\lambda_{max} = 570$ nm) and an M-like species (λ_{max} 410 nm), are increasingly populated [26]. Resonance Raman, FTIR and X-ray diffraction have confirmed that the transitions in D85N involve the same chromophore isomerizations [24,27] and structural changes [23,27], which occur in the wild-type protein during the M↔N and N↔O transitions. D85N is thus a useful system for probing the BR reprotonation mechanism.

Predicting the intermolecular interactions that regulate the conformational changes coupled to proton movement requires, at a minimum, detailed understanding of the molecular interactions of all structural states. Atomic level structures are known for the BR and M states [6,8,9,21] and lower resolution structures are available for the K and N states [28,29]. These structures illustrate the amino acid interactions that change during structural transitions. Understanding how side-chain movements regulate the pK_a's of critical proton binding and release sites requires molecular engineering and biophysical characterization. Much progress has been made in this regard via the use of site-directed mutagenesis [30], but this analysis is incomplete. An alternative approach is to utilize strategies that enable screening for interesting second-site mutations generated by the techniques of scanning, random mutagenesis, and in vitro molecular evolution [31]. While the fortuitous formation of the PM has facilitated the purification and structural analysis of site-directed mutants, this protocol would be prohibitively time-consuming when coupled with saturation mutagenesis. To address this limitation, we have developed an efficient high-throughput spectroscopic screening method that will expedite characterization of large numbers of mutants. Our approach uses reflectance spectroscopy of whole cell samples and avoids the requirement for BR purification.

2. Materials and methods

2.1. Bacterial strains

The *Escherichia coli* strain used was DH5α (F^-, *recA1*, *endA1*, *gyrA96*, *thi1*, *hsdR17* (r^-_k, m_k^+), *supE44*, 1^-). The *H. salinarum* strain used was L33 (Vac^-, Rub^-, BR^-; [18]).

2.2. Media and growth conditions

All salts and chemicals were reagent-grade. Bacteriological peptone was from Oxoid, Unipath (Hampton, England), yeast extract tryptone, Lennox Broth, and Bacto-Agar were from Difco Laboratories (Detroit, MI). Complex haloarchaeal medium was basal salts plus peptone [32]. *H. salinarum* cells were transformed as described previously [33]. Selective media included 10–25 μM mevinolin (gift from Merck, Sharp and Dohme, Rathaway, NJ). Growth of *H. salinarum* cultures was monitored using a Beckman DU-40 spectrophotometer at λ_{660}. Complex *E. coli* medium was LB medium or TY medium. *E. coli* cells were transformed by Hanahan's high efficiency calcium shock method [34]. Selective media included 50 μg/ml ampicillin (Sigma, St. Louis, MO). *E. coli* and *H. salinarum* cells were grown at 37 °C in a New Brunswick G25 shaking incubator (Edison, NJ) at 225 rpm.

2.3. Reagents

All restriction enzymes and DNA-modifying enzymes were from New England BioLabs, (Beverly, MA). Custom oligo-deoxynucleotides were synthesized by GIBCO Life Technologies (Rockville, MD), *Taq* Polymerase and deoxynucleotide triphosphates were from Perkin Elmer (Norwalk, CT) and *Pfu* Polymerase was from Stratagene (La Jolla, CA). Wizard DNA miniprep kit was from Promega Corporation (Madison WI), Qiaquick PCR purification kit was from Qiagen (Valencia, CA) and Freeze 'n Squeeze DNA gel extraction spin columns were from Bio-Rad (Hercules, CA). Electrophoresis grade agarose was from FMC Corporation (Rockland, ME).

2.4. Mutagenesis

Construction of the expression vectors containing wild-type BR and BR containing the D85N mutation has been described previously [26]. The D85N/T170C mutant was generated using in vitro gene assembly [31] described elsewhere [45].

Two second-site mutants, R82Q and D96N, were introduced into the D85N background by PCR mutagenesis. Using the pENDS:D85N vector as a template, oligos 1 and 2 (Table 1) were used to amplify a DNA fragment containing both the D85N and R82Q mutations. The product was digested with *Bam*HI and *Apa*I, purified and ligated to create the pENDS:R82Q vector. In addition to generating the R82Q mutation, oligo 1 destroys the *Bss*HII site present in the D85N gene but creates a new silent restriction site *Apa*I at amino acid positions 80–82. Successful cloning was confirmed by restriction digest analysis.

The D96N mutant [35] was cloned on a *Kpn*I/*Not*I fragment into pENDS bop I [36]. Using pENDS bop I:D96N as a template, oligos 2 and 3 (Table 1) were used to amplify a DNA fragment containing both the D85N and D96N mutations. Along with the D96N mutation, the DNA template introduces the silent restriction site *Spe*I within the codons for amino acids 99 and 100. Oligo 3 introduces the D85N mutation and the silent restriction site, *Bss*HII, within the codons for amino acids 81 and 82. The product was digested with *Bam*HI and *Bss*HII, purified, and ligated into the pENDS:D85N vector. Desired clones were identified by restriction analysis.

Each of the pENDS vectors containing the BR mutants was digested with *Pst*I and *Bam*HI. The 1.2-kb fragment containing the bacterio-opsin (*bop*) gene was subcloned into the *H. salinarum* shuttle vector, pUBP2 [37], to generate pHex expression vectors. Positive clones were confirmed by restriction digests. DNA (1.5 μg) for each of the pHex vectors containing the desired mutations was dried in a Savant Speed-Vac (Holbrook, NY) and resuspended in 15 μl of Spheroplasting Solution (0.5 M EDTA, 2 M NaCl, 27 mM KCl, 50 mM Tris–HCl, 15% sucrose) for transformation into *H. salinarum*. Following isolation of positive transformants, the *bop* gene was obtained by PCR from *H. salinarum* cell lysates and confirmed by DNA sequencing.

2.5. Cellular screen

H. salinarum cultures expressing the BR constructions were grown to late stationary phase of growth in 5 ml Rich Halo Media containing 10 μM mevinolin. Cultures were pelleted and resuspended in 1 ml of basal salts. Four 200-μl aliquots of cell suspension were transferred to a nylon membrane (Hybond N, Amersham) using a vacuum manifold, designed in-house for this purpose. To prevent crystal formation upon drying, salt was removed from the membrane by equilibrating with deionized water three times. While this procedure likely lysed the *H. salinarum* cells, the resultant whole cell pastes (e.g. total membrane and cytoplasmic fractions) were retained on the membrane. Equilibration was accomplished by immersing a blotting pad (VWR, So. Plainfeild, NJ) in water (or buffer, see below) such that the blotting pad was thoroughly wet, but not submerged. Nylon membranes were placed, sample side up on the blotting pad for 15 min. Cell samples were subsequently equilibrated in titration buffer (100 mM NaCl, 20 mM 3-[cyclohexylamino]-1-propane-sulfonic acid (CAPS), 20 mM bis tris–propane (BTP), 40 mM NaH_2PO_4) at pH 7.5, 9.0, and 10.5. The pH of the nylon membranes was checked with pH paper. Samples were allowed to dry at room temperature for 1 h before spectra were collected. Spectra were recorded at the reflectance port of an RSA 150 integration sphere (Labsphere, North Sutton, NH) coupled to a PE λ18 UV/Vis spectrophotometer (Perkin Elmer). Four spectra (350 to 800 nm) were recorded of each sample. Spectra were normalized to 0.000 A at 750 nm and smoothed using a 10-point moving average. λ_{max} values were determined using the Perkin Elmer UV WinLab software's peak finder function. The λ_{max} at each pH value was reported as an average of the λ_{max} values determined for the four spectra. The N/O peak heights were determined by plotting one normalized spectrum from each pH value on the same graph and measuring from the λ_{max} to the baseline. Percent changes were reported relative to the peak height measured at pH 7.5.

Table 1
Oligodeoxynucleotides used in BR mutagensis

Oligo No.	Sequence (5′ to 3′)
(1)	TTGGGCCCAGTACGCTGCTAACTGGCTG
(2)	AAAAGGATCCGAGTACAAGACCGAGTG
(3)	TTGCGCGCTACGCTAACTGGCTG

2.6. Purification of BR mutants

H. salinarum cultures expressing the BR mutants were grown from single colonies in 5-ml cultures with 10 μM mevinolin. Following three subcultures, a 50-ml culture with mevinolin was inoculated and grown to midlog phase (OD_{660} 0.5–0.7). This culture was used to inoculate a 1.5-l culture to an OD_{660} of 0.01. Cells were harvested, lysed, and BR purified as described previously [26]. Purified membranes were stored at −70 °C in titration buffer containing 25% sucrose.

2.7. Spectra of purified D85N:cysteine mutants

Purified high-density membranes were pelleted and washed three times in titration buffer at pH 7.2. Resuspended membranes were dark-adapted (DA) for at least 16 h at 4 °C prior to titration. All subsequent manipulations were performed under dim red light. Absorbance spectra were recorded at the diffuse transmittance port of the integration

sphere. Samples (0.5–0.8 OD/ml) were placed in a 3-ml quartz cuvette (1-cm pathlength). The cuvette holder was thermostatted at 20 °C using a Lauda RC20 circulator (Brinkmann Instruments, Westbury, NY). Samples were titrated by delivering (via a Microlab 500B dual syringe pump, Hamilton, Reno, NV) 1–5 μl of 5 N HCl or 5 N NaOH (in titration buffer) to the sample cuvette. The cuvette was then capped and inverted 15 times. Following the addition of titrant, the temperature was measured using a temperature probe (Radiometer America, Westlake, OH). When the temperature had equilibrated (steady reading for 20 s at 20 ± 0.3 °C) the pH was recorded on a Radiometer PHM240 pH meter using a Radiometer calomel electrode (pHC4000-8). At each pH value, the volume of titrant was tabulated and absorbance spectra were collected from 800 to 250 nm at 1-nm intervals (2-nm slit width).

3. Results

3.1. Whole cell screen

BR concentration in the PM was quantified using a Perkin Elmer λ18 spectrophotometer and LabSphere RSA 150-mm light scattering attachment ($\varepsilon_{568}^{BR} = 62{,}700\ M^{-1}\ cm^{-1}$; [38]). Samples for spectral measurements were prepared by dilution (in basal salts) of washed whole cells to equivalent absorbance at 410 nm. The absorbance at 410 nm is due to a membrane-associated cytochrome and is linearly proportional to the amount of total cells in the sample whether BR was expressed (Fig. 1, solid circles) or not (Fig. 1, open circles). BR accumulation was normalized to equivalent numbers of cells for comparative analysis.

We then established the ability of reflectance spectroscopy to reproduce ground-state absorbance properties characteristic of purified BR. Wild-type PM was applied to nylon filters and equilibrated at neutral pH, as described for the whole cells. For DA BR the λ_{max}, determined by reflectance spectroscopy, was 568 nm while the λ_{max} was 558 nm for light-adapted (LA) BR (Fig. 2B). The same analysis was performed for whole cells expressing wild-type BR and the λ_{max} determined were 566 ± 1 and 558 ± 3 nm for the LA and DA, respectively (Fig. 2A), demonstrating the precision and accuracy of the λ_{max} determined from whole cell pastes.

We then compared the pH-dependent absorbance properties of whole cells expressing D85N with those of PM containing purified D85N (Fig. 3). In D85N, the absorbance maximum of the spectral peak, which occurs between 550 and 650 nm ($^{550-650}\lambda_{max}$), is a weighted average of the relative concentrations of the N ($\lambda_{max} = 570$ nm) and O ($\lambda_{max} = 615$ nm) intermediates [26]. The average $^{550-650}\lambda_{max}$ values, at pH 7.5, 9.0, and 10.5, agreed closely with those obtained from purified protein (Table 2). No concentration dependence was observed in the determination of $^{550-650}\lambda_{max}$ for cells expressing D85N (data not shown). For

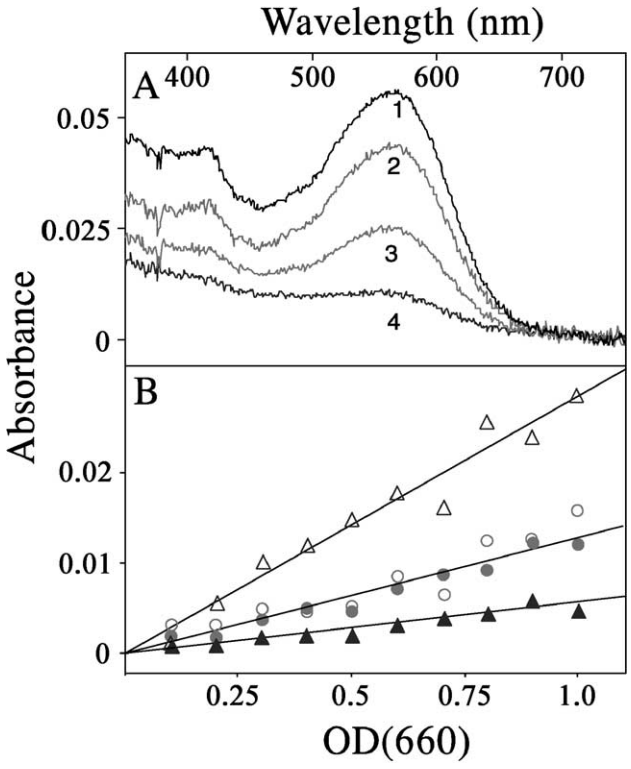

Fig. 1. Reflectance spectroscopy of whole cells. 50-ml cultures of L33 and L33 transgenically expressing BopI (wild type), were grown to stationary phase. Cell pellets were collected and washed with basal salts and resuspended to 50 ml. (A) Reflectance spectra of L33 cells expressing BopI for the following volume dilutions with basal salts: (1) undiluted, (2) 80% cell suspension:20% basal salts, (3) 40% cell suspension:60% basal salts, (4) 10% cell suspension:90% basal salts. The absorbance maximum at 568 nm is due to BR; the absorbance maximum at 410 nm is due to a membrane-associated cytochrome. (B) Reflectance measurements of dilutions of L33 (solid symbols) and L33 expressing BopI (open symbols). Triangles are measurements taken at 568 nm (BR absorbance maximum) and circles are measurements taken at 410 nm (cytochrome absorbance maximum). The cytochrome absorbance exhibits the same linear dependence with cell number in the presence or absence of BR accumulation.

the whole cell paste samples the standard deviation of the $^{550-650}\lambda_{max}$ values increased with increasing pH. This results from the M state ($\lambda_{max} = 410$ nm) becoming increasingly populated at high pH causing a decrease in amplitude and broadening of the N/O peak. The $^{550-650}\lambda_{max}$ values determined from the cell paste reflectance spectra reproduce the corresponding values determined by visible absorbance spectroscopy of PM containing purified D85N.

Subsequently, the spectral transitions of three D85N second-site mutant whole cell pastes (D85N/T170C, D85N/D96N, and D85N/R82Q) were compared with transitions obtained with purified protein (Fig. 4). Combining these mutations with the D85N mutation allowed evaluation of the homologous intermediate state transitions by ground-state reflectance spectroscopy. As shown in Fig. 4A, D85N/T170C has a red-shifted $^{550-650}\lambda_{max}$ at pH 7 and exhibits significant concentrations of the N state at all pH values. The pH dependence of the red shift is evident in the

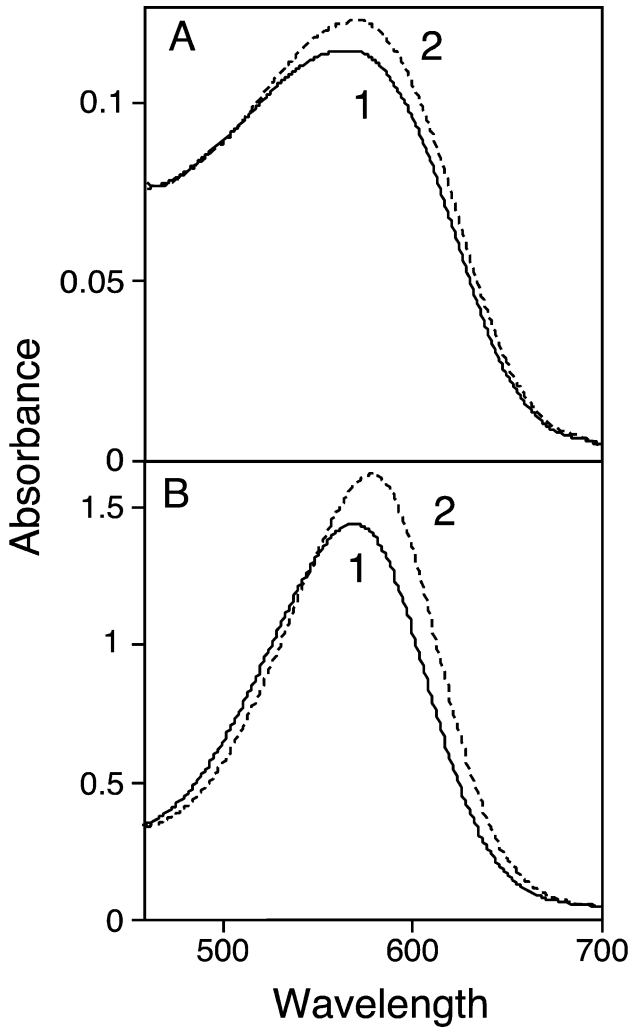

Fig. 2. Spectral changes during light-adaptation for wild-type BR. Whole cells, or purified PM, were coated on to nylon filter paper by vacuum. Samples were DA at room temperature for 5 days and subsequently LA by exposure to light greater than 500 nm for 20 min. (A) Reflectance spectra: 1, DA wild-type whole cells; 2, LA wild-type whole cells. (B) Reflectance spectra: 1, DA wild-type PM; 2, LA wild-type PM.

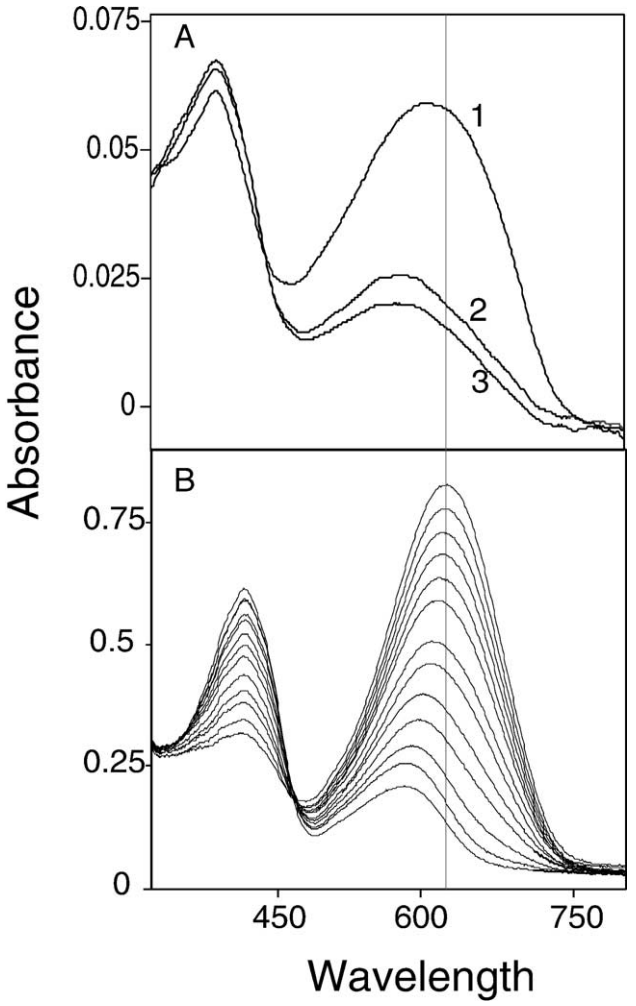

Fig. 3. pH dependence of D85N spectra changes (100 mM NaCl, 20 mM CAPS, 20 mM BTP, 20 mM, 20 mM NaH_2PO_4). (A) Reflectance spectra of DA whole cells expressing D85N: (1) pH 7.0, (2) pH 9.0, (3) pH 10.5. (B) Absorbance spectra of DA PM containing D85N. The spectra were obtained at pH 7.13 (greatest amplitude at 615 nm and lowest amplitude at 410 nm), 7.51, 7.77, 7.95, 8.15, 8.34, 8.72, 9.06, 9.50, 9.94, 10.20, 10.42, and 10.81 (lowest amplitude at 580 nm and greatest amplitude at 410 nm). The spectral changes are completely reversible (data not shown).

reflectance spectroscopy of whole cell pastes and absorbance spectroscopy of the purified protein sample.

The amino acids D96 and R82 are both located on helix C and their role in light activated proton translocation is well established through extensive study of the mutants D96N and R82Q [39–43]. The D85N/R82Q double mutant spectrum contains three spectral components in a pH-dependent equilibrium (Fig. 4B, [44]). Unlike D85N, however, the presence of two isosbestic points indicates that the spectral transitions occur with discrete pK_a values. As the pH is increased, the blue shift in the N/O peak occurs first, followed by a decrease in amplitude, and the accumulation of an absorbance peak at 410 nm (M). At neutral pH, the $^{550-650}\lambda_{max}$ determined from whole cells expressing D85N/R82Q was very similar to that previously reported for purified protein (e.g. 579 and 582 nm, respectively [44]). This $^{550-650}\lambda_{max}$, at neutral pH, is not as red-shifted as that of D85N (Fig. 3, 610 nm), indicating that the O and N species are both significantly populated at pH 7. At pH 9.0, the whole cell spectrum was blue-shifted relative to the spectrum at pH 7.5, consistent with increased accumulation of N. The increase in amplitude of the M peak, however, was only observed in the spectrum recorded at pH 10.5 and above (Fig. 4B). The cell paste reflectance spectra demonstrated that $^{550-650}\lambda_{max}$ of D85N/D96N only shifted by 10 nm as the pH was increased from 7.5 to 10.5, compared to a

Table 2
Comparison of λ_{max} (nm) values determined by reflectance spectroscopy of whole cell pastes and purified protein samples

D85N sample	pH 7.5	pH 9.0	pH 10.5
Whole cells	615 ± 1	594 ± 4	582 ± 7
Purified protein	613	595	571

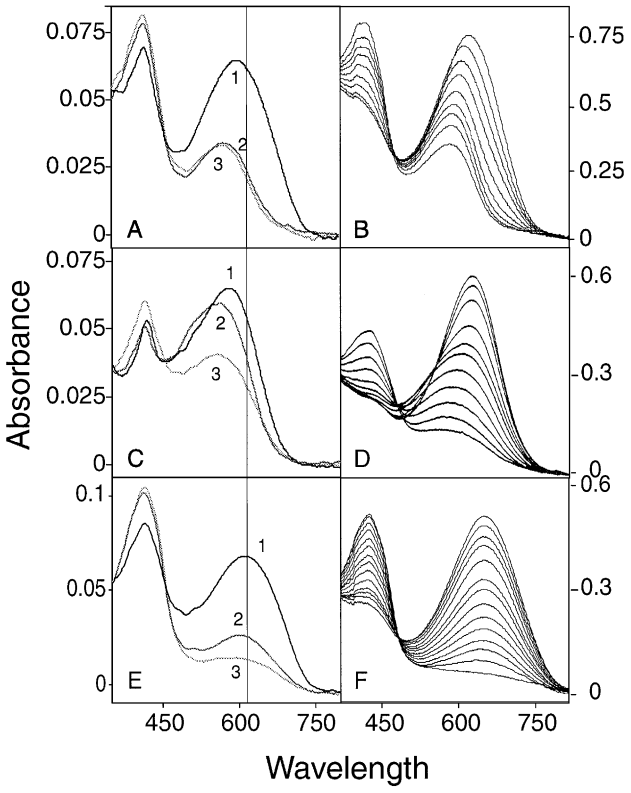

Fig. 4. pH dependence of D85N second-site mutant absorbance spectra in 100 mM NaCl, 20 mM CAPS, 20 mM BTP, 20 mM, 20 mM NaH_2PO_4. (A) Reflectance spectra of DA whole cells expressing D85N/T170C; (1) pH 7.0, (2) pH 9.0, (3) pH 10.5. (B) Absorbance spectra of DA PM containing D85N/T170C. The spectra were obtained at pH 7.28 (greatest amplitude at 615 nm and lowest amplitude at 410 nm), 7.52, 7.90, 8.00, 8.48, 9.03, 9.50, 9.92, 10.46, and 11.02. (C) Reflectance spectra of DA whole cells expressing D85N/R82Q; (1) pH 7.0, (2) pH 9.0, (3) pH 10.5. (D) Absorbance spectra of DA PM containing D85N/R82Q. The spectra were obtained at pH 7.11, 7.51, 8.02, 8.54, 8.93, 9.24, 9.70, 10.12, 10.90, and 11.22. (E) Reflectance spectra of DA whole cells expressing D85N/D96N; (1) pH 7.0, (2) pH 9.0, (3) pH 10.5. (F) Absorbance spectra of DA PM containing D85N/D96N. The spectra were obtained at pH 6.75, 7.26, 7.45, 7.75, 8.05, 8.22, 8.44, 8.86, 9.08, 9.22, 9.53, 9.75, and 10.97.

32-nm shift in D85N (Fig. 4B). The change in N/O peak height is ~10%, greater for D85N/D96N than for D85N, consistent with increased M accumulation in the double mutant.

4. Discussion

We have developed a cell paste reflectance screen to expedite the analysis of the numbers of BR mutants that can be generated by random and semi-random mutagenesis. This report demonstrates the precision and accuracy achieved by ground-state reflectance analysis of solid samples, prepared from as little as 5 ml of cell culture, and without the need for BR purification. We first validated the approach by analysis of the LA and DA states of wild-type BR and then by analysis of pH-dependent ground-state transitions of four site-directed mutants, D85N, D85N/T170C, D85N/D96N, and D85N/R82Q.

We used the single-site BR mutant D85N to probe ground-state transitions that are close homologues of the reprotonation phase of light-induced proton pumping [26,45]. The protonation-state of aspartate 85 plays a central role in the conformational changes and linked proton movements. The use of the D85N mutant was the key since the neutral side chain group of D85 effectively "permanently" protonated D85. Uncoupling the pK_a of D85 from the BR mechanism restricted the available conformational space to transitions that normally contained a protonated D85. In the absence of photoexcitation, homologues of the M, N, and O states exist in equilibrium and their relative concentrations are sensitive to bulk solvent proton activity. At neutral pH, D85N exists as an O-like species (blue in color). As the pH is raised, two additional chromophoric species, an N-like species (purple in color) and an M-like species (yellow in color), become populated at high pH [26]. Thus, in the ground-state, the D85N mutant has trapped homologues of the M, N, and O intermediates. The intermediate state transitions of the single-site mutants T170C, D96N, R82Q exhibit defects in the reprotonation mechanism, and we anticipate that similar defects will be observed with these mutations in the background of the D85N transitions.

Reflectance spectra of D85N/T170C whole cell pastes indicate significant N accumulation at neutral pH. Indeed, N is apparent at all pH. Threonine 170 is located in the F helix and its side chain participates in forming the cytoplasmic proton channel at the level of the position of D96. In the reprotonation phase of the photocycle, D96 donates its proton to the Schiff base during the decay of M. Mutations in the cytoplasmic side of the proton channel have previously been shown to effect the kinetics of N formation, possibly by altering the hydration of the channel and D96 [46]. The single-site mutations T49V, F219L, and F171C decreased the pK_a of D96 so that the ground-state conformation exhibits N-like character [47]. In addition, maleimide-labeled T170C possessed a photocycle characterized by accelerated M decay and slow decay of N resulting in its accumulation [46,48]. The transitions observed in the whole cell pastes containing D85N/T170C correspond well with spectral phenotypes previously reported and support the hypothesis that amino acid interactions in the cytoplasmic portion of the proton channel regulate the pK_a of D96 and the accumulation of N (Fig. 4, [44,49,50]).

Reflectance analysis of D85N/R82Q demonstrates that a purple (N) and yellow (M) species form at pH values similar to those observed for the purified material [44] and the accumulation of N and M proceed with different pK_a's (e.g. two isosbestic points are evident in the spectral transitions, Fig. 4). In the single-site mutant D85N, M and N are in rapid equilibrium and the transition between them is pH-independent (Martinez and Turner, unpublished), consistent with the observation of a single isosbestic point (Fig. 3). R82 is situated a hydrophilic pocket of the extramembranous half-

channel and in numerous BR structures has been identified at variable distances from D85, D212, E204, and structured waters [5–8,29,51]. Consistent with its potential for forming a multitude of intramolecular contacts, R82 plays a number of critical roles in light-induced BR proton transduction. Mutation of R82 has been shown to affect the linkage between the pK_a's of D85 and the PRG(s) in both the ground and M states [44,52]. In the ground-state the R82Q mutation raised the pK_a of D85 from ~2.2 to near 7 and lead to significant accumulation of a blue species [40,42,53,54]. R82A and R82Q were shown to have reduced proton pumping efficiencies and a perturbed rate for the back reaction from N to M. The D85N/R82Q ground-state transitions identified a defect that corresponds closely with that observed in photo-kinetic studies and indicates a role for R82 in the accumulation of the M state.

Following photoexcitation, at neutral pH, the D96N single-site mutant has a slow M decay resulting in accumulation of the M intermediate [41]. X-ray diffraction of D85N/D96N revealed that, at neutral pH, the double mutant has a conformation like that of D85N at alkaline pH [49] (e.g. an M homologue is present in both mutants). Unlike D85N, the N intermediate does not form as the pH is raised [24,55]. We therefore predicted that no shift in the $^{550-650}\lambda_{max}$ would be observed as pH was increased in the reflectance spectra of D85N/D96N whole cell pastes. In addition, due to the decrease in the pK_a of the Schiff base, M was predicted to accumulate at lower pH values. The whole cell reflectance analysis is consistent with both predictions and supports the need for D96 deprotonation in the accumulation of the N state.

In sum, there is a clear phenotypic consensus on comparing spectral phenotypes of PM containing purified BR and the reflectance spectroscopy of the whole cell pastes. The phenotypes assigned to the D85N second-site mutants using the whole cell reflectance spectra correspond closely to the phenotypes reported previously for both single- and double-site mutants. This not only supports the use of the whole cell reflectance spectra to monitor BR conformational transitions; it illustrates the correspondence between the ground-state pH-dependent transitions of D85N and the analogous photocycle transitions of wild-type BR. Owing to the small amount of sample required and the lack of requirement for BR purification, this reflectance technique would be very useful in high-throughput screening of large numbers of BR mutants that can be generated by random and semi-random mutagenesis. We have exploited ground-state transitions of BR to establish this technique at equilibrium. In principle, the technique can be modified for time-resolved applications and our future effort will focus on that potential.

Spectroscopy of whole cell preparations will be useful as a rapid screen for high-level protein expression by eliminating the need for extensive pre-processing of samples. Unfortunately, the scattering component dominates the UV region of the reflectance spectroscopy so that useful chromophoric signatures will only be available in the visible and IR regions. This approach will have immediate application to screening and quantitative analysis of microbial cultures, producing proteins with endogenous chromophores such as cytochromes, or proteins that can be derivatized with exogenous chromophores during preparation of cell pastes. Indeed, recent work by McGovern et al. [56] demonstrated that quantitative analysis of protein expression from *E. coli* cell pastes could be accomplished by a combination of various spectroscopy and "supervised learning" methodologies. A major conclusion of that work was that application of multivariate analytical methods allowed reliable quantification from spectra that had significant contributions from components other than the target species. The system we describe takes advantage of the intense absorbance of BR in the visible absorbance region such that modeling is not required for species quantification. We have recently demonstrated the utility of this cell paste-reflectance strategy by analysis of the pH-dependent spectral transition of 59 BR mutants, generated during a cysteine-scanning mutagenesis of two of the seven BR transmembrane helices [45].

Acknowledgements

Support is gratefully acknowledged in the form of an American Heart Association Grant-in-Aid (AHA664871), the National Science Foundation (MCB-9817140), a Johnson and Johnson Focused Giving Program Grant, and American Heart Association Predoctoral Fellowships (AHA9804168V and 0010097B) to LCM.

References

[1] D. Oesterhelt, W. Stoeckenius, Proc. Natl. Acad. Sci. U. S. A. 70 (1973) 2853–2857.
[2] D. Oesterhelt, W. Stoeckenius, Methods Enzymol. 31 (1974) 667–678.
[3] A.M. Winter-Vann, L. Martinez, L. Parker, J. Talbot, G.J. Turner, Cancer Res. Ther. Control 8 (1999) 275–289.
[4] R. Henderson, Annu. Rev. Biophys. Bioenerg. 6 (1977) 87–109.
[5] R. Henderson, J.M. Baldwin, T.A. Ceska, F. Zemlin, E. Beckman, K.H. Downing, J. Mol. Biol. 213 (1990) 899–929.
[6] E. Pebay-Peyroula, G. Rummel, J.P. Rosenbusch, E.M. Landau, Science 277 (1997) 1676–1681.
[7] Y. Kimura, D.G. Vassylyev, A. Miyazawa, A. Kidera, M. Matsushima, K. Mitsuoka, K. Murata, T. Hirai, Y. Fujiyoshi, Nature 389 (1997) 206–211.
[8] H. Luecke, B. Schobert, H.T. Richter, J.P. Cartailler, J.K. Lanyi, J. Mol. Biol. 291 (1999) 899–911.
[9] S. Subramaniam, R. Henderson, Biochim. Biophys. Acta 1460 (2000) 157–165.
[10] R. Mathies, C. Brito-Cruz, W. Pollard, C. Shank, Science 240 (1988) 777–779.
[11] R.H. Lozier, R.A. Bogomolni, W. Stoeckenius, Biophys. J. 15 (1975) 955–962.
[12] D. Oesterhelt, J. Tittor, Trends Biochem. Sci. 14 (1989) 57–61.
[13] G. Varo, A. Duschl, J.K. Lanyi, Biochemistry 29 (1990) 3798–3804.
[14] G. Varo, J.K. Lanyi, Biochemistry 30 (1991) 5008–5015.

[15] M.P. Krebs, H.G. Khorana, J. Bacteriol. March 1993 (1993) 1555–1560.
[16] S.P. Balashov, Biochim. Biophys. Acta 1460 (2000) 75–94.
[17] E. Racker, W. Stoeckenius, Biol. Chem. 249 (2) (1974) 662–663.
[18] G. Wagner, D. Oesterhelt, G. Krippahl, J. Lanyi, FEBS Lett. 131 (1983) 341–345.
[19] G. Varo, J.K. Lanyi, Biochemistry 34 (1995) 12161–12169.
[20] H.J. Sass, I.W. Schachowa, G. Rapp, M.H. Koch, D. Oesterhelt, N.A. Dencher, G. Buldt, EMBO J. 16 (1997) 1484–1491.
[21] H.J. Sass, G. Buldt, R. Gessenich, D. Hehn, D. Neff, R. Schlesinger, J. Berendzen, P. Ormos, Nature 406 (2000) 649–653.
[22] T. Mogi, L.J. Stern, T. Marti, B.H. Chao, H.G. Khorana, Proc. Natl. Acad. Sci. 29 (1988) 4148–4152.
[23] L.S. Brown, H. Kamikubo, L. Zimanyi, M. Kataoka, F. Tokunaga, P. Verdegem, J. Lugtenburg, J.K. Lanyi, Proc. Natl. Acad. Sci. U. S. A. 94 (1997) 5040–5044.
[24] L.S. Brown, A.K. Dioumaev, R. Needleman, J.K. Lanyi, Biochemistry 37 (1998) 3982–3993.
[25] H. Kandori, Y. Yamazaki, M. Hatanaka, R. Needleman, L.S. Brown, H.T. Richter, J.K. Lanyi, A. Maeda, Biochemistry 36 (1997) 5134–5141.
[26] G.J. Turner, L. Miercke, T. Thorgeirsson, D. Kliger, M.C. Betlach, R.M. Stroud, Biochemistry 32 (1993) 1332–1337.
[27] A. Nilsson, P. Rath, J. Olejnik, M. Coleman, K.J. Rothschild, J. Biol. Chem. 270 (1995) 29746–29751.
[28] P.A. Bullough, R. Henderson, J. Mol. Biol. 286 (1999) 1663–1671.
[29] J. Vonck, EMBO J. 19 (2000) 2152–2160.
[30] L.S. Brown, Biochim. Biophys. Acta 1460 (2000) 49–59.
[31] W.P.C. Stemmer, Nature 370 (1994) 389–391.
[32] S. DasSarma, E.M. Fleischmann, in: F.T. Robb (Ed.), Archaea, A Laboratory Manual, vol. 3, Cold Spring Harbor Laboratory Press, Cold Spring Harbor, 1995, pp. 1–280.
[33] S.W. Cline, W.L. Lam, R.L. Charlebois, L.C. Schalkwyk, W.F. Doolittle, Can. J. Microbiol. 35 (1989) 148–152.
[34] D. Hanahan, J. Jessee, F.R. Bloom, Methods Enzymol. 204 (1991) 63–113.
[35] R.F. Shand, L.J.W. Miercke, A.K. Mitra, S. Fong, R.M. Stroud, M.C. Betlach, Biochemistry 30 (1991) 3082–3088.
[36] G.J. Turner, R. Reusch, A.M. Winter-Vann, L. Martinez, M.C. Betlach, Protein Expr. Purif. 17 (1999) 312–323.
[37] U. Blaseio, F. Pfeifer, Proc. Natl. Acad. Sci. U. S. A. 87 (1990) 6772–6776.
[38] M. Rehorek, M.P. Heyn, Biochemistry 18 (1979) 4977–4983.
[39] Y. Cao, G. Varo, A.L. Klinger, D.M. Czajkowsky, M.S. Braiman, R. Needleman, J.K. Lanyi, Biochemistry 32 (1993) 1981–1990.
[40] L.J.W. Miercke, M.C. Betlach, A.K. Mitra, R.F. Shand, S.K. Fong, R.M. Stroud, Biochemistry 30 (1991) 3088–3098.
[41] H. Otto, T. Marti, M. Holz, T. Mogi, M. Lindau, H.G. Khorana, M.P. Heyn, Proc. Natl. Acad. Sci. U. S. A. 86 (1989) 9228–9232.
[42] S.P. Balashov, R. Govindjee, M. Kono, E. Imasheva, E. Lukashev, T.G. Ebrey, R.K. Crouch, D.R. Menick, Y. Feng, Biochemistry 32 (1993) 10331–10343.
[43] M.S. Hutson, U. Alexiev, S.V. Shilov, K.J. Wise, M.S. Braiman, Biochemistry 39 (2000) 13189–13200.
[44] L.S. Brown, L. Bonet, R. Needleman, J.K. Lanyi, Biophys. J. 65 (1993) 124–130.
[45] L.C. Martinez, R.L. Thurmond, P.G. Jones, G.J. Turner, Proteins: Struct., Funct., Genet. (2002) in press.
[46] L.S. Brown, G. Varo, R. Needleman, J.K. Lanyi, Biophys. J. 69 (1995) 2103–2111.
[47] S. Subramaniam, M. Lindahl, P. Bullough, A.R. Faruqi, J. Tittor, D. Oesterhelt, L. Brown, J. Lanyi, R. Henderson, J. Mol. Biol. 287 (1999) 145–161.
[48] M. Pfeiffer, T. Rink, K. Gerwert, D. Oesterhelt, H.J. Steinhoff, J. Mol. Biol. 287 (1999) 163–171.
[49] M. Kataoka, H. Kamikubo, F. Tokunaga, L.S. Brown, Y. Yamazaki, A. Maeda, M. Sheves, R. Needleman, J.K. Lanyi, J. Mol. Biol. 243 (1994) 621–638.
[50] L.S. Brown, A.K. Dioumaev, R. Needleman, J.K. Lanyi, Biophys. J. 75 (1998) 1455–1465.
[51] K. Takeda, H. Sato, T. Hino, M. Kono, K. Fukuda, I. Sakurai, T. Okada, T. Kouyama, J. Mol. Biol. 283 (1998) 463–474.
[52] S.P. Balashov, R. Govindjee, E.S. Imasheva, S. Misra, T.G. Ebrey, Y. Feng, R.K. Crouch, D.R. Menick, Biochemistry 34 (1995) 8820–8834.
[53] L. Stern, P. Ahl, T. Marti, T. Mogi, M. Duñach, S. Berkowitz, K. Rothschild, H.G. Khorana, Biochemistry 28 (1989) 10035–10042.
[54] S. Subramaniam, T. Marti, H.G. Khorana, Biophysics 87 (1990) 1013–1017.
[55] J. Tittor, U. Schweiger, D. Oesterhelt, E. Bamberg, Biophys. J. 67 (1994) 1682–1690.
[56] A.C. McGovern, R. Ernill, B.V. Kara, D.B. Kell, R. Goodacre, J. Biotechnol. 72 (1999) 157–167.